ISSN NO. 2320-5407

Journal homepage: http://www.journalijar.com

INTERNATIONAL JOURNAL OF ADVANCED RESEARCH

RESEARCH ARTICLE

A Simulated Climatology of North African Dust and its Impact on Meteorological Parameters Using WRF-CHEM Model

***A. A. Abdallah[1], M. M. Eid[1], Abdel Wahab M. M.[2] and F. M. El-Hussainy[1]**

1. Astronomy and Meteorology Department, Faculty of Science, Al-Azhar University, Cairo, Egypt.
2. Astronomy and Meteorology Department, Faculty of Science, Cairo University, Giza, Egypt.

Manuscript Info

Manuscript History:

Received: 15 November 2015
Final Accepted: 22 December 2015
Published Online: January 2016

Key words:
WRF-Chem simulation,
Climate dust Simulation,
North African dust simulation,
impact of dust on meteorological parameters

****Corresponding Author***

A. A. Abdallah.

Abstract

The climatic effects of dust outbreaks in North Africa have been simulated using the weather research and forecasting model coupled with chemistry module (WRF-CHEM). This work presents the second simulation (climate dust simulation) of a series of simulations (first was climate simulation (2m Temperature and Precipitation) and the third will be aerosols climate simulation) with WRF-CHEM model over a large domain covering most of the African continent. The Ozone Monitoring Instrument (OMI) absorbing Aerosol Index (AI) is used to indicate the presence of elevated absorbing aerosol (such as desert dust) in the earth's atmosphere. For the distribution of dust concentration, the WRF-CHEM model captured the distribution of dust concentration over the studied area according to the OMI absorbing aerosol index AI. For the impact of dust on the meteorological parameters we got the seasonal differences (DUSTRUN-NODUST) for 2m temperature, precipitation, outgoing longwave radiation (OLR), and cloud fraction, the climate simulation including dust generally reduces the precipitation in the normal rainfall band over North Africa, as well as overall seasons due to the dusty case, OLR is reduced over the mostly cloudy North Africa region, while the cloud fraction shows decreases across North Africa and the Atlantic with an increase to the east, and the differences in T2m varied from season to season. The increase in precipitation is associated with increased convection in that region due to the heating of the air column by dust particles, as well as produces more cooling at the cloud top.

Introduction:-

Over the last years full attention has been given to the modelling of aerosols by the scientific community with a special emphasis on Saharan dust outbreaks [1][2]. It is known that dust outbreaks can travel long distances, and that high amounts of dust are transported above the mixing layer at a typical height between four to five kilometers in the free troposphere, often in a thin plume that can grow up to one kilometer thick [3][4], having affect, directly and indirectly, the atmospheric radiative budget. Moreover, the study of dust outbreaks becomes of high interest as these particles can interact with solar and thermal radiation, perturbing the Earth's radiative budget, with consequent impacts on climate [5][6] and also changing cloud microphysical properties by acting as cloud condensation nuclei [7][8]. In addition, dust is also important for air quality through its impact on visibility and human health [9].

Among the different components of aerosols in the atmosphere, wind-blown dust is emitted in large quantities over arid and semi-arid regions. Mineral dust, from both natural and anthropogenic sources, is the most abundant atmospheric aerosol component in terms of aerosol dry mass, contributing more than half of the total global aerosol burden [10]. Major sources of dust are located in arid regions, including deserts, semi-arid deserts, dry lake beds and ephemeral channels, where annual rainfall is extremely low [11] and substantial amounts of alluvial sediment have been accumulated [12].

Northern Africa is characterized by a Mediterranean climate at the north coast and a large desert area in the south, where temperatures are the hottest [13]. According to global climate projections [14], the already environmentally stressed Middle East and North Africa region will be one of the most prominent climate change hotspots. Substantial decreases in precipitation, especially during the winter season and intense warming, most pronounced during summer, will probably have strong economic and societal impacts in the region [15]. The Sahara desert over North Africa is the largest source of mineral dust in the world; mineral dust can modify the hydrological cycle over North Africa and modulate the tropical North Atlantic temperature [16]. Since finer dust particles can be lifted to high altitudes, where they are transported over long distances (often thousands of kilometers) from the source regions, Saharan dust can also play an important role in modifying climate on the global scale, when transported northward across the Mediterranean region up to central and northern Europe, or westward across the Atlantic Ocean occasionally to the eastern coast of the United States [17][18].

In addition to these natural sources, human-induced droughts, disturbance of the land surface and climate variability (i.e. the anthropogenic sources for mineral dust) have also contributed to an increase of mineral dust aerosols within the atmosphere [19]. Additionally, mineral dust has a significant influence on the climate system directly by scattering and absorbing solar and infrared radiation [20], semi-directly through changes in atmospheric temperature structure and evaporation rate of cloud droplets (i.e. the cloud burning effect; [21], and indirectly in a complex way through impact on optical properties of clouds (i.e. enhancing cloud reflectance by increasing total droplet cross-sectional area; [22].

The relationship between atmospheric processes and dust aerosols is bidirectional, so that while the atmosphere can have a major impact on dust entrainment and its three-dimensional distribution, dust aerosols in turn can have impacts on the atmosphere. It has also been noted that direct radiative forcing by mineral dust changes the vertical profile of temperature and atmospheric stability, which in turn influences the wind speed profile within the lower atmosphere [23]. Previous studies indicate that mineral dust aerosols cool the surface and lower atmosphere, and warm the dust layer above during daytime [23], thereby contributing to establishing a more stable atmosphere [24], and hence decreasing near-surface wind speed [25][26], but increasing winds in layers above [23]. Such disturbance in meteorological fields may change the emission and transport of dust particles [27].

This article is an effort to simulate the regional climate dust over a large domain covering most of the African continent, especially North Africa using WRF-CHEM model, as well as the impact of climate dust on some meteorological parameters. In general, this work is the second simulation (dust concentration only) of a series of climate simulations over North Africa, the first simulation studied the regional climate simulation of WRF model over North Africa [28], and the third will be the climate aerosols simulation.

Model, Data and Experimental Design:-

a. Regional WRF-Chemistry Model:-

The Weather Research and Forecasting (WRF) system is a mesoscale forecast model with an incorporated data assimilation capability that advances both the understanding and prediction of weather [29]. WRF has been utilized in a variety of research and operational projects, from the scale of convective storms to the scale of continental weather patterns [30]. WRF-Chem extends WRF by incorporating a chemistry module that interactively simulates emissions of aerosols and gases, their transport, turbulent and convective mixing, and chemical and microphysical transformations of trace gases and aerosols [31].

The WRF-Chem version 3.5 was used for this dust simulation. The WRF-Chem model generates the dust emissions during the actual run. The "online" dust emissions data is provided through land usage information produced by the WRF Preprocessing system (WPS) and the simulated meteorological fields. The land use categories based on the United States Geological Survey's (USGS) land use/cover system as shown in Fig. 1(a). In this study, the GOCART (Goddard Global Ozone Chemistry Aerosol Radiation and Transport) simple aerosol scheme was used, as this study only focuses on the simulation of dust particles. Five discrete size bins of dust particles were considered, with idealized spherical shapes whose radii range from 0.1 to 8.0 mm. The five dust bins in the model are 0.5:1, 1.4:2, 2.4:3, 4.5:4 and 5:8.0 um, with corresponding effective radii of 0.5, 1.4, 2.4, 4.5, and 8.0 mm.

The GOCART dust scheme considers preferential sources based on erodible fraction [32] and calculates the vertical dust flux from the surface as [33][34]. Dust emission flux is controlled by the surface properties (such as soil composition (clay, silt, and sand), see Fig. 1(c and d) for clay and sand fractions, vegetation, and soil moisture content), and surface wind velocity [35]. The dust emission flux in each bin is size-resolved, which is calculated by taking into account the soil particle fraction, erosion factor, see Fig. 1(e), surface wind velocity, and the threshold velocity of wind erosion.

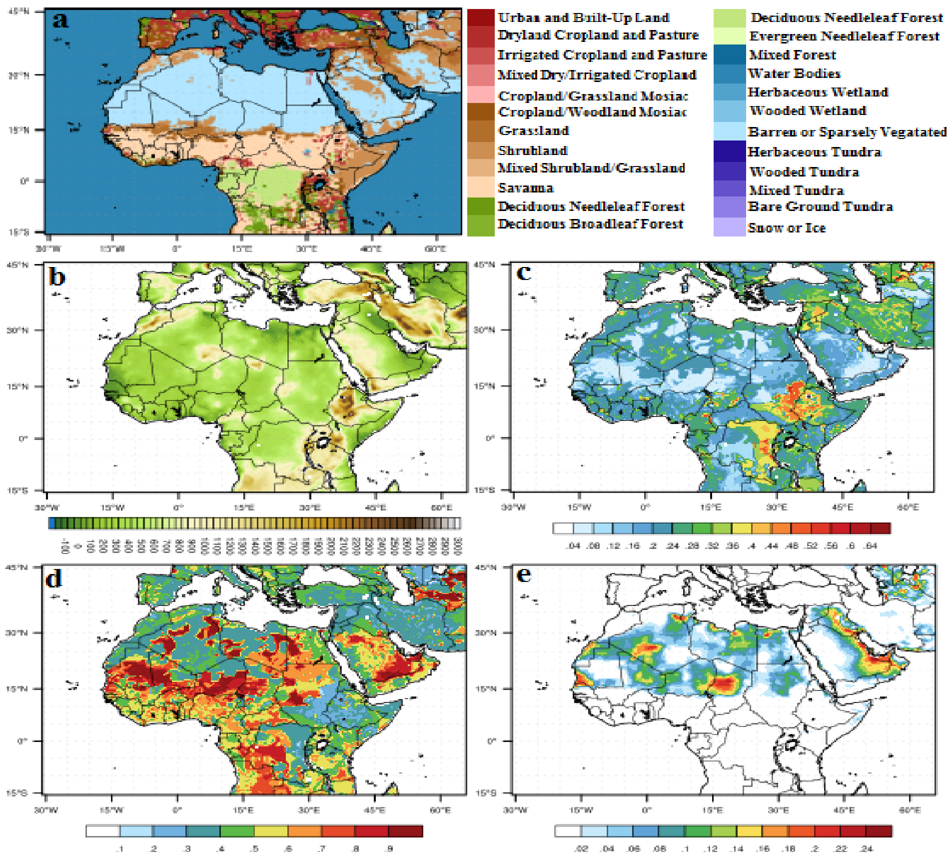

Fig. 1: a) Land use categories for the domain used, **b)** Terrain height of model domain over African continent with a 50-km resolution grid, the Soil fraction of **c)** Clay and **d)** Sand from the soil categories data that are provided as part of WPS static data, and **e)** Fraction of erodible surface.

b. Data Forcing:-

The reanalysis data that provide the initial and lateral boundary conditions to the regional climate WRF-Chem model in this study is the NCEP/DOE Reanalysis-2 global data [36]. This data was created in cooperation between the National Centers for Environmental Prediction (NCEP) and Department of Energy (DOE). NCEP/DOE Reanalysis-2 is an improved version of the NCEP Reanalysis-1 model that fixed errors and updated parameterizations of physical processes. The NCEP/DOE Reanalysis-2 data are split into 2D and 3D files, the 2D data has T63 horizontal spectral resolution (1.875 × 1.875 degrees) while 3D has horizontal spectral resolution (2.5 × 2.5 degrees), the temporal coverage is 4-times daily and monthly values, and 17 vertical levels, with the top extending to 10 hPa. The global SST data used has weekly of temporal coverage and (1 × 1 degrees) horizontal resolution and updated in the model every 6 hr.

The Ozone Monitoring Instrument (OMI) Ultra-Violet Aerosol Index (AI) product will be used to indicate the presence of elevated absorbing aerosol (such as desert dust) in the earth's atmosphere. The concept of the UV aerosol index (AI) was first introduced in the context of observations made by the Total Ozone Mapping Spectrometer (TOMS) sensors in the late 1990s [37] and has since been extended to apply to measurements with the Ozone Monitoring Instrument (OMI). OMI is a Dutch–Finnish instrument onboard the NASA EOS Aura spacecraft [38] launched in July 2004. OMI is the successor of the TOMS instruments and is dedicated to the monitoring of the Earth's ozone, air quality and climate. It is a useful qualitative parameter for detecting the presence of absorbing aerosols in the atmosphere, based on a spectral contrast method in the near-UV region where ozone absorption is very small [37][39]. One interesting aspect of this parameter is that it is directly derived from instrument measurements and consequently is not affected by uncertainties in assumed aerosol properties.

i. Experimental Design:-

In our simulation the physics options include the Lin et al. Microphysics scheme [40], Kain–Fritsch convective parameterization scheme [41], CAM Shortwave and Longwave schemes [42], the Yonsei University planetary boundary layer scheme [43], the Noah Land Surface Model (LSM) four-layer soil temperature and moisture model with canopy moisture and snow-cover prediction [44], MM5 Similarity Surface Layer Scheme [45][46] and the GOCART simple dust aerosol scheme [33][34]. A summary of the selected model physics and chemistry options is given in Table 1. The extent of the North Africa domain is presented in **Fig. 1(b)**, while the length of the simulation is 5.5 years (July 2006-December 2011), in addition to five months of spin-up time (July-November 2006) which was excluded from our analysis. We have used a horizontal resolution of 50 km and 51 vertical levels. The NCEP/DOE reanalysis-2 dataset was used to provide initial and boundary conditions, and covered the most African continent (including the North Africa interior domain). The output is stored every 6 h (00, 06, 12, 18 UTC) and monthly fields are therefrom derived.

Table 1: The model physics options used.

Compartment	***Selected scheme(s)***
Microphysics	Lin et al
Long wave radiation	CAM
Short wave radiation	CAM
Planetary boundary layer	YSU
Land surface	Noah LSM
Convective parameterization	Kain–Fritsch (KF)
Dust Emission	GOCART Scheme (Ginoux et al., 2001)

As mentioned before, this work will focus on the distribution of dust concentration and its impact on some meteorological parameters (such as Temperature at 2m, Precipitation, Cloud cover, Outgoing longwave radiation). For the distribution of dust concentration, the OMI-AI will be used to indicate the presence of elevated absorbing aerosol (such as desert dust) in the earth's atmosphere and will compare between the surface dust concentration and the OMI-AI. Dust detection in the near UV band is possible using the OMI-AI which is a measure of the change of spectral contrast in the near UV due to radiative transfer effects of aerosols. The OMI-AI can be considered to be proportional to the dust burden, so it is a good indication of the dust spatial pattern, and as such it can be used for model validation. NON-absorbing aerosols (e.g., sulfate aerosols and sea-salt particles) yield negative AI values. UV-absorbing aerosols (e.g., dust, smoke, and biomass burning) yield positive AI values. Clouds yield near-zero values. In this paper we deal only with absorbing aerosols; henceforth, we refer to the positive values from (1) as the absorbing aerosol index. The comparison focused on the monthly mean of the surface dust concentration and the OMI-AI. Moreover, monthly observations derived from the OMI-AI dataset were used for 8 selected locations over the desert area in North Africa domain for the trends of mean surface dust concentration. Table 2 shows the stations location in their countries.

For the impact of dust on the meteorological parameters, the WRF model output in the first simulation (climate simulation) [28] will be used, for the meteorological parameters used we subtract the first run (climate simulation) from the second run (climate dust simulation), e.g. [DUSTRUN-NODUAT] over the seasonal mean of the simulation period.

Table 2: The 8 stations location in their countries over the study domain

Countries	***Station location***
Chad	Bodele
Cape Verde	Cape Verde
Algeria	Bordj-Bodji Mokhtar and Tamanrasset
Morocco	Dahkla
Egypt	El-Farafra
Mali	Agoufou
Niger	Banizoumbou

Results:-

In this section the model surface dust concentration outputs are compared with the OMI-AI dataset while the next section will discuss the process of subtract of the meteorological parameters for the dust simulation and the simulation without dust.

a. Dust Concentration

The monthly mean of OMI-AI for the period of 2007-2011 is presented in the first and third column panel of Fig. 2 (a-c, g-i), and Fig. 3 (a-c, g-i), while the second and fourth column panel Fig. 2 (d-f, j-l), and Fig. 3 (d-f, j-l) for the distribution of surface dust concentration from the WRF model. Using the OMI absorbing Aerosol Index, it was found that the most important sources of dust aerosols are located in the Northern Hemisphere, primarily over the Sahara and Sahel in North Africa; the Bodélé Depression (17°N, 18°E, 170 m) of the northern Lake Chad Basin in North Africa is the most intense source of dust in the world.

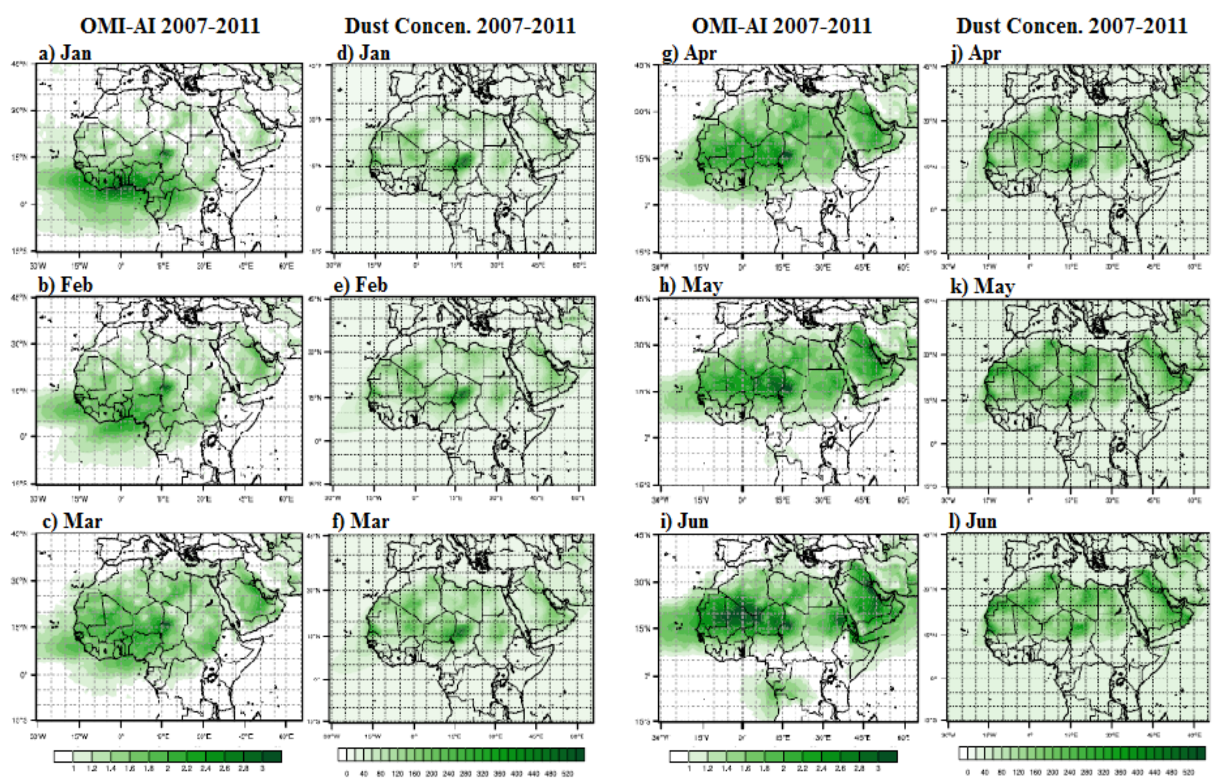

Fig. 2: The monthly mean of OMI-AI for the period of 2007-2011 in the left column panel of a) January, b) February, c) March, g) April, h) May, and i) June, and the surface dust concentration (ug/kg-dryair) in right column panel of d) January, e) February, e) March, i) April, j) May, and k) June.

The second intense source of dust in North Africa was identified in the West Sahara, east of the Mauritanian coast near the Mali Mauritanian border stretching northeast towards the Mali-Algerian boarder. Other smaller sources include south of the northern (Tell) Atlas Mountains in northern Algeria, the eastern Libyan Desert, and the Nubian Desert in Egypt and Sudan. Note that high OMI-AI values along the coast of the Gulf of Guinea near the western coast of Africa (in months of winter and spring), as well as over southern Africa region (in austral winter and spring months) are attributed to biomass burning and smoke. In general, the WRF-Chem model captured the distribution of dust concentration over the studied area according to the OMI absorbing aerosol index AI.

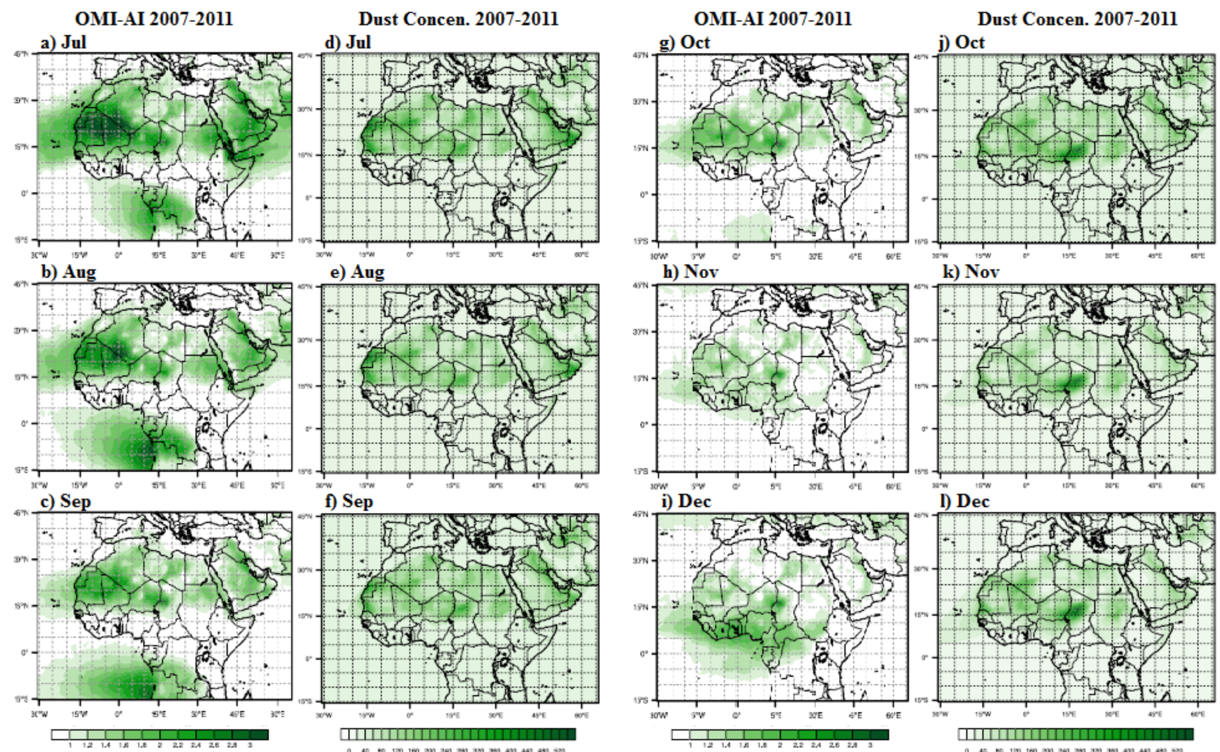

Fig. 3: Same as Fig. 2 but in the left column panel of a) July, b) August, c) September, g) October, h) November, and i) December, and the right column panel of d) July, e) August, e) September, i) October, j) November, and k) December.

Stations Comparison:-

A comparison between surface dust concentration of WRF-Chem model simulation and the OMI-AI data was performed over 8 station locations (Table 2) over the study domain as shown in Fig. 4. The closest model land grid point to the stations coordinates is considered with the mean AI of the closest OMI grid point for the comparisons. Fig.4 present the monthly averages of the positive values of the OMI-derived AI from 2007 to 2011 for the pixels corresponding to the 8 station locations. The highest AI values appear at Bodele, Cape Verde, Bordj-Brodji-Mokhtar, Dahkla, Agoufou, and Banizoumbou (with maximum value beyond 3). Similarly, the highest monthly mean surface dust concentrations are obtained at the same months as AI values. Overall the dust concentration values of WRF-Chem model matches best with the peak of maximum values of the OMI-AI for the most of the 8 stations.

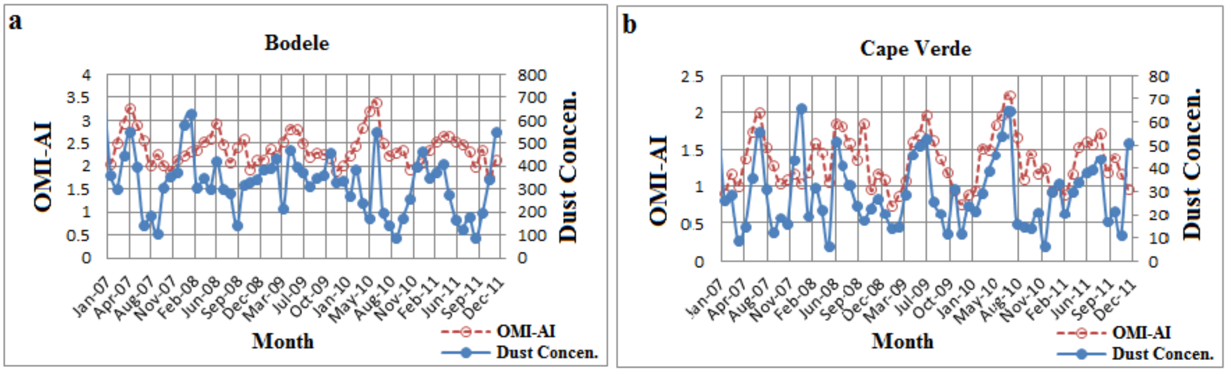

Fig. 4: The time series of the monthly averages of the positive values of the OMI-AI and of modeled surface dust concentration (ug/kg-dryair) from 2007-2011 for **a)** Bodele and **b)** Cape Verde**.**

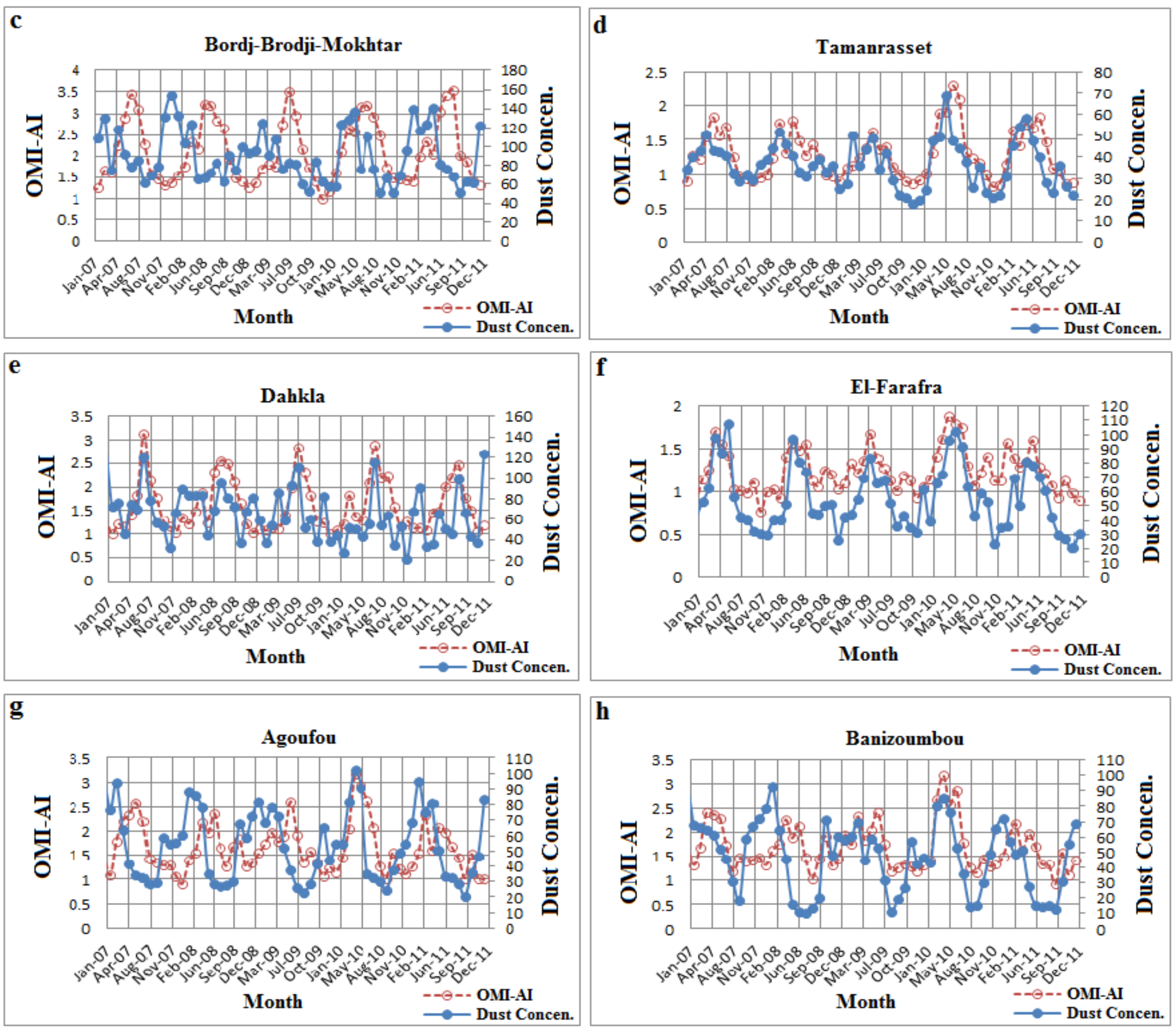

Fig. 5: same as Fig. 4 but for **c)** Bordj-Brodji Mokhtar, **d)** Tamanrasset, **e)** Dahkla, **f)** El-Farafra, **g)** Agoufou, and **h)** Banizumbou**.**

Meteorological Parameters:-

In accordance with our research objective, we have performed a series of simulations (3 simulations: the first for climate simulation [28], the second for climate dust simulation (this work), and the third for climate aerosol simulation (future work)), each simulation is a 5.5-yr run with the initial condition corresponding to 1 July (climatologically). The meteorological forces are fixed in all simulations so that dust emission is the only varying forcing between first and second simulation in this study. This section will show the impact of dust outbreak force on the meteorological parameters (e.g. 2m temperature, precipitation, outgoing longwave radiation, and cloud fraction) by comparing the 5-years simulation results of the first and second simulations. Differences between first and second simulation show the sensitivity of dust modulated on meteorological parameters due to the dust emissions in North Africa as shown in Fig. 6 and Fig. 7.

The seasonal mean differences in 2m temperature are presented in the top panel of Fig. 6 and the bottom panel for differences in precipitation. During the DJF season, the 2m temperature is increased over the North African band especially over Egypt, Libya, Algeria, Tunisia, north of Sudan, Niger, and Chad (above latitude of 10^{o}N), while the

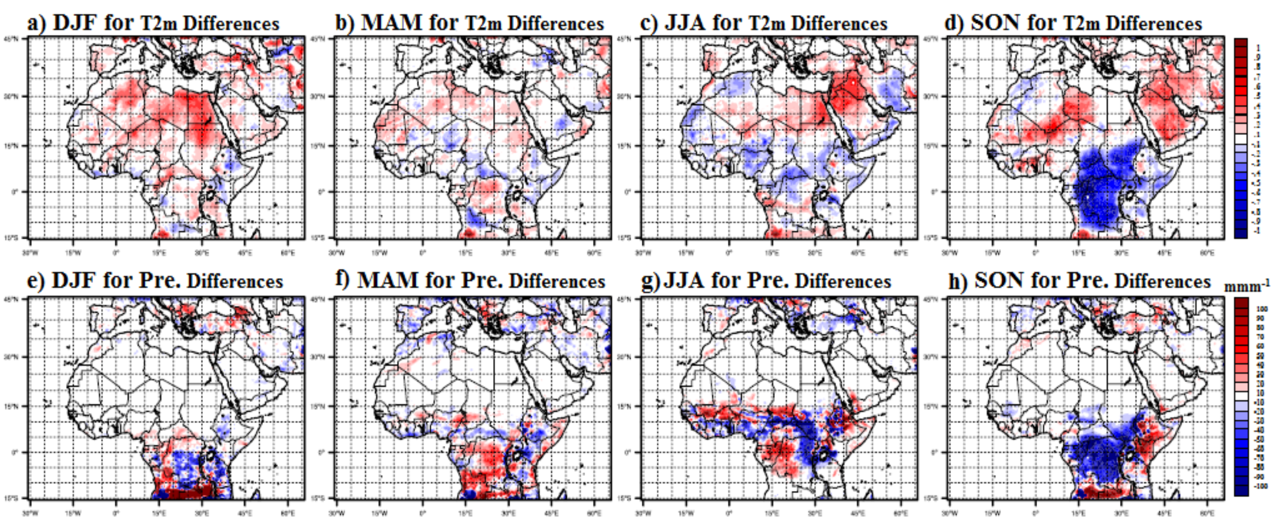

Fig. 6: The seasonal mean differences in temperature at 2m **a)** DJF, **b)** MAM, **c)** JJA, and **d)** SON and precipitation **e)** DJF, **f)** MAM, **g)** JJA, and **h)** SON**.**

T2m decreased over Ethiopia as shown in Fig. 6a. The rainfall system in North Africa could be significantly affected by dust particles; it's decreased over Ethiopia, Democratic Republic of Congo, Uganda, Rwanda, and Burundi as shown in Fig. 6e. Fig. 6b shows the MAM difference in T2m, the values of T2m are decreased over some parts of Mali, Niger, south of Chad, Ethiopia, and north of Central Africa Republic, while the T2m increased over north of Sudan, Egypt, Libya, Algeria, Tunisia, and Mauritania. For precipitation in MAM as in Fig. 6f, it's values are increased over Democratic Republic of Congo, Angola, south of Chad, north of Nigeria, and eastern of Algeria, while decreased over Ethiopia, north of Central Africa Republic, Tunisia, and Morocco.

During the JJA season as in Fig. 6c, the T2m decreased over north of Algeria, Mauritania, Mali, south of Niger, Nigeria, Chad, Ethiopia, and Central Africa Republic, while increased over Egypt, Libya, north of Niger, south of Algeria, and west coast of Morocco. Fig. 6g shows the JJA differences in precipitation, the values decreased over east and north coasts of Congo, Central Africa Republic, and Nigeria while the values increased over south of Chad, west and south coasts of Nigeria, south of Mali. For the SON differences in T2m, the values increased over parts of Libya, Algeria, Mali, and Niger as shown in Fig. 6d while decreased south of Sudan, south of Chad, Central Africa Republic, and middle of Africa. Fig. 6h shows the SON differences in precipitation that the values decreased over south of Sudan, south of Chad, Central Africa Republic, and Congo while the values increased over Ethiopia.

The seasonal mean differences in outgoing longwave radiation are presented in the top panel of Fig. 6 and the bottom panel for differences in cloud fraction.

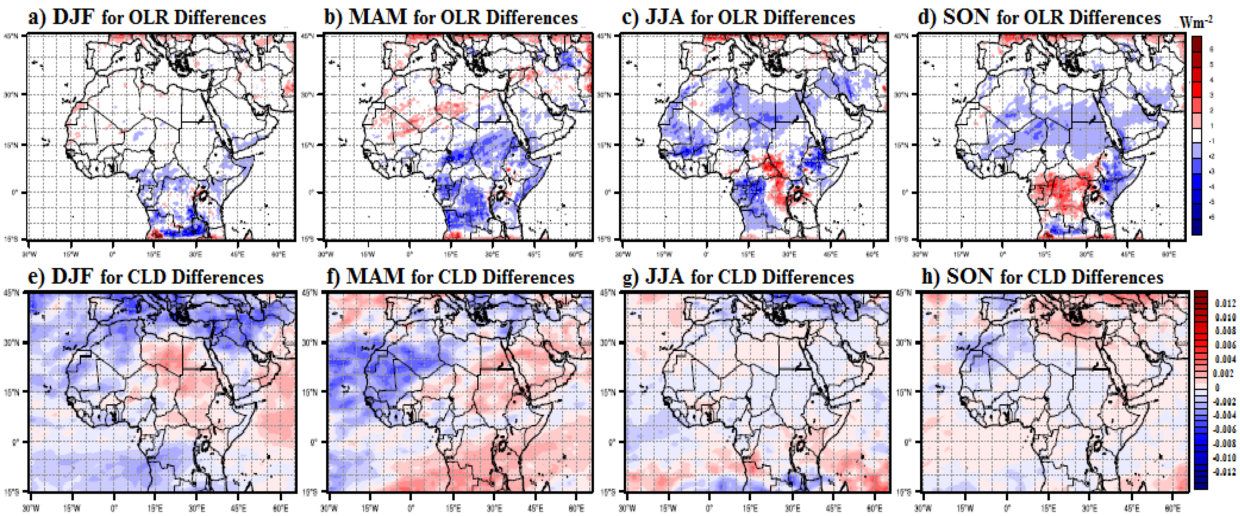

Fig. 7: The seasonal mean differences in OLR **a)** DJF, **b)** MAM, **c)** JJA, and **d)** SON and cloud fraction **e)** DJF, **f)** MAM, **g)** JJA, and **h)** SON**.**

Overall seasons as shown in Fig. 7(a-d), due to the dusty case, OLR is reduced over the mostly cloudy North Africa region. Precipitation in the same area, however, increases Fig. 6(e-h), corresponding to the enhanced convection as indicated by reduced OLR, while the cloud cover shows decreases across North Africa and the Atlantic with an increase to the east Fig. 7(e-h). Adding the dust effect in the model simulation reduces the precipitation in the normal rainfall band over North Africa. The increase in precipitation is associated with increased convection in that region due to the heating of the air column by dust particles, as well as produces more cooling at the cloud top. The differences between adding the dust emissions in the second simulation and the first simulation are indicating that the dust emissions forces play a dominant role in the overall climatic effect over North Africa.

Conclusions and Future Work:-

While Numerous RCMs have been developed and applied for simulating the dust climate in the worldwide locations, we used the climate-chemistry version of WRF model to conduct the dust climate simulation over North African domain. This simulation is the second from a series of simulations; the first was for the climate simulation and the third will be for climate aerosols simulation.

The results of 5.5 years climate dust simulation have been carried out to study the distribution of dust concentration and its impact on the 2m temperature, outgoing longwave radiation, cloud field, and precipitation patterns over North African domain. The WRF-Chem simulation for dust succeeds in reproducing the main geographical distribution and monthly variations of surface dust concentration in comparing to OMI absorbing aerosol index.

For the impact of dust on the meteorological parameters we found that, the climate simulation including dust generally reduces the precipitation in the normal rainfall band over North Africa, as well as overall seasons due to the dusty case, OLR is reduced over the mostly cloudy North Africa region, while the cloud cover shows decreases across North Africa and the Atlantic with an increase to the east, and the differences in T2m varied from season to season. The increase in precipitation is associated with increased convection in that region due to the heating of the air column by dust particles, as well as produces more cooling at the cloud top.

The future work including aerosols simulation, will conduct using WRF-Chem model in climate mode for the same period and configuration.

References:-

[1] Pey, J., Querol, X., Alastuey, A., Forastiere, F., Stafoggia, M. (2013). African dust outbreaks over the mediterranean basin during 2001{2011: Pm 10 concentrations, phenomenology and trends, and its relation with synoptic and mesoscale meteorology. Atmospheric Chemistry and Physics 13 (3), 1395-1410.

[2] Laken, B. A., Parviainen, H., Pall_e, E., Shahbaz, T. (2014). Saharan mineral dust outbreaks observed over the north atlantic island of la palma in summertime between 1984 and 2012. Quarterly Journal of the Royal Meteorological Society 140 (680), 1058-1068.

[3] Guerrero-Rascado, J. L., Olmo, F., Avil_es-Rodr__guez, I., Navas-Guzma_n, F., P_erez-Ram__rez, D., Lyamani, H., Alados-Arboledas, L. (2009). Extreme saharan dust event over the southern Iberian peninsula in september 2007: active and passive remote sensing from surface and satellite. Atmos. Chem. Phys 9 (21), 8453-8469.

[4] Yang, W., Marshak, A., Va_rnai, T., Kalashnikova, O. V., Kostinski, A. B. (2012). Calipso observations of transatlantic dust: vertical strati_cation and e_ect of clouds. Atmospheric Chemistry and Physics 12 (23), 11339-11354.

[5] Santos, D., Costa, M. J., Silva, A. M., Salgado, R. (2013). Modeling saharan desert dust radiative effects on clouds. Atmospheric Research 127, 178-194.

[6] Anton, M., Valenzuela, A., Mateos, D., Alados, I., Foyo-Moreno, I., Olmo, F., Alados-Arboledas, L. (2014). Longwave aerosol radiative e_ects during an extreme desert dust event in southeastern spain. Atmospheric Research.

[7] Weinzierl, B., Sauer, D., Esselborn, M., Petzold, A., Veira, A., Rose, M., Mund, S., Wirth, M., Ansmann, A., Tesche, M., et al. (2011). Microphysical and optical properties of dust and tropical biomass burning aerosol 448 layers in the cape verde regionan overview of the airborne in situ and lidar measurements during samum-2. Tellus B 63 (4), 589-618.

[8] Alam, K., Trautmann, T., Blaschke, T., Subhan, F. (2014). Changes in aerosol optical properties due to dust storms in the middle east and southwest asia. Remote Sensing of Environment 143, 216-227.

[9] Thomson, M.C., Molesworth, A.M., Djingarey, M.H., Yameogo, K.R., Belanger, F., Cuevas, L.E. (2006). Potential of environmental models to predict meningitis epidemics in Africa. Trop. Med. Int. Health 11 (6), 781–788. http://dx.doi.org/10.1111/j.1365-3156.2006.01630.x.

[10] Textor, C., Schulz, M., Guibert, S., Kinne, S., Balkanski, Y., Bauer, S., Berntsen, T., Berglen, T., Boucher, O., Chin, M., Dentener, F., Diehl, T., Easter, R., Feichter, H., Fillmore, D., Ghan, S., Ginoux, P., Gong, S., Kristjansson, J., Krol, M., Lauer, A., Lamarque, J., Liu, X., Montanaro, V., Myhre, G., Penner, J., Pitari, G., Reddy, S., Seland, O., Stier, P., Takemura, T., Tie, X. (2006). Analysis and quantification of the diversities of aerosol life cycles within AeroCom. Atmos. Chem. Phys. 6 (7), 1777–1813.

[11] Goudie, A.S., Middelton, N.J. (2006). Desert Dust in the Global System. Springer.

[12] Ginoux, P.A., Prospero, J.M., Gill, T.E., Hsu, C., Zhao, M. (2012). Global-scale attribution of anthropogenic and natural dust sources and their emission rates based on MODIS Deep Blue aerosol products. Rev. Geophys. 50, RG3005. http://dx.doi.org/10.1029/2012RG000388.

[13] World Meteorological Organization, the climate in Africa (2013), (WMO-No. 1147**), 015.**

[14] Van Oldenborgh, G.J., Collins, M., Arblaster, J., Christensen, J.H., Marotzke, J., Power, S.B., Rummukainen, M.T. and Zhou, T. (2013) Annex I: Atlas of Global and Regional Climate Projections. In: Stocker, T.F., Qin, D., Plattner, G.K., Tignor, M., Allen, S.K., Boschung, J., Nauels, A., Xia, Y., Bex, V. and Midgley, P.M., Eds., Climate Change 2013: The Physical Science Basis, Contribution of Working Group I to the Fifth Assessment Report of the Intergovernmental Panel on Climate Change, Cambridge University Press, Cambridge, and New York.

[15] Lelieveld, J., Hadjinicolaou, P., Kostopoulou, E., Chenoweth, J., Maayar, M., Giannakopoulos, C., Hannides, C., Lange, M.A., Tanarhte, M., Tyrlis, E. and Xoplaki, E. (2012). Climate Change and Impacts in the Eastern Mediterranean and the Middle East. Climatic Change, **114**, 667-687. http://dx.doi.org/10.1007/s10584-012-0418-4

[16] Lau, K. M., Kim, K. M., Sud, Y. C., and Walker, G. K. (2009). AGCM study of the response of the atmospheric water cycle of West Africa and the Atlantic to Saharan dust radiative forcing, Ann. Geophys., 27, 4023–4037, doi:10.5194/angeo-27-4023-2009.

[17] Chin, M., Diehl, T., Ginoux, P., and Malm, W. (2007). Intercontinental transport of pollution and dust aerosols: implications for regional air quality, Atmos. Chem. Phys., 7, 5501–5517, doi:10.5194/acp-7-5501-2007.

[18] Flaounas, E., Coll, I., Armengaud, A., and Schmechtig, C. (2009). The representation of dust transport and missing urban sources as major issues for the simulation of PM episodes in a Mediterranean area, Atmos. Chem. Phys., 9, 8091–8101, doi:10.5194/acp-9-8091-2009.

[19] Tegen, I., Werner, M., Harrison, S.P., Kohfeld, K.E. (2004). Relative importance of climate and land use in determining present and future global soil dust emission. Geophys. Res. Lett. 31, L05105. http://dx.doi.org/10.1029/2003GL019216.

[20] Miller, R.L., Tegen, I. (1998). Climate response to soil dust aerosols. J. Clim. 11 (12), 3247–3267.

[21] Koren, I., Kaufman, Y.J., Remer, L.A., Kaufman, Y.J., Remer, L.A., Koren, I., Martins, J.V., Martins, J.V. (2004). Measurement of the effect of Amazon smoke on inhibition of cloud formation. Science 303 (5662), 1342–1345. http://dx.doi.org/10.1126/science.1089424.

[22] Su, J., Huang, J., Fu, Q., Minnis, P., Ge, J., Bi, J. (2008). Estimation of Asian dust aerosol effect on cloud radiation forcing using Fu-Liou radiative model and CERES measurements. Atmos. Chem. Phys. 8 (10), 2763–2771. http://dx.doi.org/10.5194/acp-8-2763-2008.

[23] Alizadeh Choobari, O., Zawar-Reza, P., Sturman, A. (2012b). Feedback between windblown dust and planetary boundary-layer characteristics: sensitivity to boundary and surface layer parameterizations. Atmos. Environ. 61, 294–304. http://dx.doi.org/10.1016/j.atmosenv.2012.07.038.

[24] Miller, R.L., Tegen, I., Perlwitz, J. (2004b). Surface radiative forcing by soil dust aerosols and the hydrologic cycle. J. Geophys. Res. 109, D04203. http://dx.doi.org/10.1029/2004JD004912.

[25] Jacobson, M.Z., Kaufman, Y.J. (2006). Wind reduction by aerosol particles. Geophys. Res. Lett. 33, L24814. http://dx.doi.org/10.1029/2006GL027838.

[26] Heinold, B., Tegen, I., Schepanski, K., Hellmuth, O. (2008). Dust radiative feedback on Saharan boundary layer dynamics and dust mobilization. Geophys. Res. Lett. 35 (20), L20817. http://dx.doi.org/10.1029/2008GL035319.

[27] Yue, X., Wang, H.J., Liao, H., Fan, K. (2010). Simulation of dust aerosol radiative feedback using the GMOD: 2. Dust-climate interactions. J. Geophys. Res. 115 (D4), D10202. http://dx.doi.org/10.1029/2008JD010995.

[28] A. A. Abdallah, M. M. Eid, Abdel Wahab M. M., F. M. El-Hussainy, (2015). Regional Climate Simulation of WRF Model over North Africa: Temperature and Precipitation, World Environment, p-ISSN: 2163-1573 e-ISSN: 2163-1581, **5**, 160-173, doi:10.5923/j.env.20150504.04.

[29] Skamarock, W.C., Klemp, J. B., Dudhia, J., Gill, D. O., Barker, D. M., Duda, M. G., Huang, X.-Y., Wang, W., Powers, J.G. et al. (2008). A Description of the Advanced Research WRF Version 3, NCAR/TN–475+STR, NCAR TECHNICAL NOTE, June 2008

[30] Michalakes, J., Duhia, D., Gill, D., Henderson, T., Klemp, J., and Wang, W. (2005). The weather research and forecast model: software architecture and performance, in: Proceedings of the 11th ECMWF Workshop on the Use of High Performance Computing in Meteorology, edited by: Zwieflhofer, W. and Mozdzynski, G., World Scientific, Singapore, 156–168.

[31] Grell, G. A., Peckham, S. E., Schmitz, R., McKeen, S. A., Frost, G., Skamarock, W. C., and Eder, B. (2005). Fully coupled online chemistry within the WRF model, Atmos. Environ., 39, 6957–6975.

[32] Cavazos Guerra, C. D. C. (2011). Modelling the Atmospheric Controls and Climate Impact of Mineral Dust in the Sahara Desert. PhD Thesis. University College London, London.

[33] Ginoux, P., Chin, M., Tegen, I., Prospero, J. M., Holben, B., Dubovik, O., and Lin, S. J. (2001). Sources and distributions of dust aerosols simulated with the GOCART model, J. Geophys. Res., 106, 20255–20273.

[34] Ginoux, P., Prospero, J., Torres, O., and Chin, M. (2004). Long-term simulation of global dust distribution with the GOCART model: correlation with the North Atlantic Oscillation, Environ. Modell. 15 Softw., 113–128.

[35] Grini, A., Myhre, G., Zender, C.S. and Isaksen, I.S.A. (2005). Model Simulations of Dust Sources and Transport in the Global Atmosphere: Effects of Soil Erodibility and Wind Speed Variability. J. Geophys. Res. 110: D02205, doi: 10.1029/2004JD005037.

[36] M. Kanamitsu, W. Ebisuzaki, J. Woollen, S-K Yang, J.J. Hnilo, M. Fiorino, and G. L. Potter. 1631-1643, Nov (2002). Bulletin of the American Meteorological Society.

[37] Torres, O., Bhartia, P. K., Herman, J. R., Ahmad, Z., and Gleason, J. (1998). Derivation of aerosol properties from satellite measurements of backscattered ultraviolet radiation: theoretical basis, J. Geophys. Res., 103, 17099–17110.

[38] Levelt, P. F., Hilsenrath, E., Leppelmeier, G. W., van den Oord, G. H. J., Bhartia, P. K., Tamminen, J., de Haan, J. F., and Veefkind, J. P. (2006). Science objectives of the Ozone Monitoring Instrument, IEEE T. Geosci. Remote, 44, 1199–1208, doi:10.1109/TGRS.2006.872336.

[39] Torres, O., Tanskanen, A., Veihelmann, B., Ahn, C., Braak, R., Bhartia, P. K., Veefkind, P., and Levelt, P. (2007). Aerosols and surface UV products from Ozone Monitoring Instrument observations: an overview, J. Geophys. Res., 112, D24S47, doi:10.1029/2007JD008809.

[40] Lin, Yuh–Lang, Richard D. Farley, and Harold D. Orville. (1983). Bulk Parameterization of the Snow Field in a Cloud Model. *J.Climate Appl. Met.*, **22**, 1065–1092.

[41] Kain, John S. (2004). The Kain–Fritsch convective parameterization: An update. *J. Appl. Meteor.*, **43**, 170–181.

[42] Collins, William D., et al. (2004). Description of the NCAR Community Atmosphere Model (CAM 3.0). NCAR Tech. Note NCAR/TN–464+STR. 214 pp.

[43] Hong, Song–You, Yign Noh, Jimy Dudhia, (2006). A new vertical diffusion package with an explicit treatment of entrainment processes. *Mon. Wea. Rev.*, **134**, 2318–2341.

[44] Tewari, M., F. Chen, W. Wang, J. Dudhia, M. A. LeMone, K. Mitchell, M. Ek, G. Gayno, J. Wegiel, and R. H. Cuenca, (2004). Implementation and verification of the unified NOAH land surface model in the WRF model. *20th conference on weather analysis and forecasting/16th conference on numerical weather prediction*, pp. 11–15.

[45] Beljaars, A.C.M. (1994). The parameterization of surface fluxes in large-scale models under free convection. *Quart. J. Roy. Meteor. Soc.*, **121**, 255–270.

[46] Zhang, D.–L., and R.A. Anthes, (1982). A high–resolution model of the planetary boundary layer– sensitivity tests and comparisons with SESAME–79 data. *J. Appl. Meteor.*, **21**, 1594–1609.